

updated June 6, 2021

1
2
3
4
5
6
7
8
9
10
11
12
13
14
15
16
17
18
19
20
21
22
23
24
25
26
27
28

Brief Research Report

Expression of the ACE2 virus entry protein in the nervus terminalis reveals the potential for an alternative route to brain infection in COVID-19

Katarzyna Bilinska¹, Christopher S. von Bartheld^{2*} and Rafal Butowt^{1*}

¹ L. Rydygier Collegium Medicum, Nicolaus Copernicus University, Bydgoszcz, Poland

² Department of Physiology and Cell Biology, University of Nevada, Reno School of Medicine, Reno, NV, United States

* Corresponding authors:

Christopher S. von Bartheld, cvonbartheld@med.unr.edu

Rafal Butowt, r.butowt@cm.umk.pl

Number of words in text: 3,984

Number of Figures: 4

Number of Tables: 0

Supplemental Figures: 1

Supplemental Tables: 2

Key words: Nervus terminalis, ACE2, SARS-CoV-2, COVID-19, brain infection, olfactory system, cathepsin

29 **Abstract**

30

31 Previous studies suggested that the SARS-CoV-2 virus may gain access to the brain
32 by using a route along the olfactory nerve. However, there is a general consensus that
33 the obligatory virus entry receptor, angiotensin converting enzyme 2 (ACE2), is not
34 expressed in olfactory receptor neurons, and the timing of arrival of the virus in brain
35 targets is inconsistent with a neuronal transfer along olfactory projections. We
36 determined whether nervus terminalis neurons and their peripheral and central
37 projections should be considered as a potential alternative route from the nose to the
38 brain. Nervus terminalis neurons in postnatal mice were double-labeled with antibodies
39 against ACE2 and two nervus terminalis markers, gonadotropin-releasing hormone
40 (GnRH) and choline acetyltransferase (CHAT). We show that a small fraction of CHAT-
41 labeled nervus terminalis neurons, and the large majority of GnRH-labeled nervus
42 terminalis neurons with cell bodies in the region between the olfactory epithelium and
43 the olfactory bulb express ACE2 and cathepsins B and L. Nervus terminalis neurons
44 therefore may provide a direct route for the virus from the nasal epithelium, possibly
45 via innervation of Bowman's glands, to brain targets, including the telencephalon and
46 diencephalon. This possibility needs to be examined in suitable animal models and in
47 human tissues.

48 **INTRODUCTION**

49 Many previous reports have suggested that the severe acute respiratory syndrome
50 coronavirus 2 (SARS-CoV-2) gains access to the brain by using an olfactory route from
51 the nose to the brain (Bougakov et al., 2020; Briguglio et al., 2020; Butowt and Bilinska,
52 2020; Li et al., 2020; Natoli et al., 2020; Meinhardt et al., 2021; Zubair et al., 2021;
53 Burks et al., 2021), similar to some other neuro-invasive viruses that are known to
54 infect olfactory receptor neurons and spread from these first-order olfactory neurons to
55 secondary and tertiary olfactory targets in the brain (Barnett and Perlman, 1993; van
56 Riel et al., 2015; Dubé et al., 2018). Indeed, it has been shown that SARS-CoV-2 can
57 accumulate in various brain regions, in animal models (reviewed in: Butowt and von
58 Bartheld, 2020; Rathnasinghe et al., 2020; Butowt et al., 2021) and in a small number
59 of human patients with COVID-19 (Ellul et al., 2020; Matschke et al., 2020; Meinhardt
60 et al., 2021; Mukerji and Solomon, 2021; Solomon, 2021; Thakur et al., 2021).

61
62 However, the route along the olfactory nerve from the nose to the brain is controversial
63 for SARS-CoV-2, primarily for two reasons: (1) the olfactory receptor neurons do not
64 express the obligatory virus entry receptor, angiotensin-converting enzyme 2 (ACE2),
65 or expression is restricted to a very small subset of these neurons (Butowt and von
66 Bartheld, 2020; Cooper et al., 2020; Brechbühl et al., 2021; Butowt et al., 2021).
67 Because sustentacular cells tightly enwrap olfactory receptor neurons (Liang, 2020),
68 these ACE2-expressing support cells can easily be mistaken for olfactory receptor
69 neurons, resulting in false positive identification. (2) The timeline of appearance of
70 SARS-CoV-2 in the brain is inconsistent with a “neuron-hopping” mode: infection of
71 third-order olfactory targets should occur with a significant delay after infection of the
72 olfactory epithelium, as has been reported for other neuro-invasive viruses (Barnett et
73 al., 1995), but instead the hypothalamus and brainstem are reported to be infected as
74 early as, or even earlier than, the olfactory bulb (de Melo et al., 2021; Zheng et al.,
75 2020), and SARS-CoV-2 may even skip the olfactory nerve and olfactory bulb on its
76 way to brain infection (Winkler et al., 2020; Zhou et al., 2020; Carossino et al., 2021).
77 These findings have raised doubt about the notion that the olfactory nerve serves as a
78 major conduit for brain infection in COVID-19 (Butowt et al., 2021).

79

80 With few exceptions (Briguglio et al., 2020; Butowt and von Bartheld, 2020; Butowt et
81 al., 2021), studies suggesting an olfactory route for SARS-CoV-2 to achieve brain
82 infection fail to consider the potential for an alternative route from the nose to the brain,
83 the route via the nervus terminalis. Many peripheral processes of the nervus terminalis
84 innervate the olfactory epithelium, the blood vessels below this epithelium, as well as
85 cells in Bowman's glands (Larsell, 1950), and the central processes of some of these
86 neurons extend to various targets in the forebrain as far caudal as the hypothalamus
87 (Pearson, 1941; Larsell, 1950; Schwanzel-Fukuda et al., 1987; Demski, 1993; von
88 Bartheld, 2004). Some of the nervus terminalis neurons are in direct contact with
89 spaces containing cerebrospinal fluid (CSF) in the region of the olfactory nerve and
90 bulb (Jennes, 1987). About 30-40% of the neurons of the nervus terminalis express
91 gonadotropin-releasing hormone (GnRH), and some of these neurons may release
92 GnRH into blood vessels below the olfactory epithelium (Jennes, 1987; Schwanzel-
93 Fukuda et al., 1987), while other neuronal populations of the nervus terminalis system
94 are thought to regulate blood flow and blood pressure in the nose and forebrain
95 (Larsell, 1918; Oelschläger et al., 1987; Ridgway et al., 1987). These properties make
96 the nervus terminalis a strong candidate for expression of ACE2, which is known to
97 regulate blood flow and blood pressure in many tissues (Tikellis and Thomas, 2012).
98 Expression of ACE2 in the nervus terminalis would suggest that this cranial nerve is a
99 plausible alternative to the olfactory nerve for the SARS-CoV-2 virus to gain access to
100 the brain. However, it has not been previously examined and reported whether nervus
101 terminalis neurons express the obligatory viral entry receptor, ACE2, and any other
102 virus entry proteases such as TMPRSS2 and cathepsins B and L. We have therefore
103 examined whether these entry proteins are expressed in nervus terminalis neurons in
104 an animal model, the postnatal mouse.

105 **MATERIALS AND METHODS**

106

107

108 **Animals and tissue processing**

109 A total of eight wildtype C57BL/6J mice (Jackson Laboratory) at age 3-4 weeks old
110 were used to obtain tissues for experiments. Mice were housed with a 12/12 hours
111 light/dark cycle and given access to water and food ad libitum. All animal experiments
112 were approved by the local ethics committee for animal research at Bydgoszcz
113 (Poland). Immediately after cervical dislocation, the mice were exsanguinated and
114 tissues were dissected. Olfactory epithelium and brain were frozen at -80°C for
115 storage and further usage, or fixed for 3 hours at 4°C in 4% (w/v) freshly prepared
116 paraformaldehyde in phosphate-buffered saline (PBS, pH 7,5), and then incubated in
117 25% (w/v) sucrose/PBS at 4°C for 16–24 hours, frozen in Tissue-Tek O.C.T. (Sakura
118 Finetek), and cryosectioned at 10-12 μm using a Leica CM1850 cryostat.

119

120 **ACE2 $-/-$ knockout (ACE2 KO) control**

121 To verify the specificity of the ACE2 antibody, an ACE2 knock-out (KO) mouse line
122 was obtained from Taconic (strain #18180). Two male homozygous ACE2 KO mice at
123 age 3 weeks old were processed and immunolabeled as described below for wildtype
124 mice. Genotyping was performed according to the manufacturer's suggested PCR
125 protocol. Lack of an ACE2 protein band was confirmed by using Western blots as
126 described previously (Bilinska et al., 2020). In brief, tissue was homogenized on ice in
127 N-Per Total Protein Extraction reagent (Thermo Scientific) with addition of protease
128 and phosphatase inhibitor cocktails (Sigma-Aldrich). Homogenates were centrifuged
129 for 30 minutes at 20,000 g at 4°C and supernatants were collected. Protein content
130 was measured by the BCA method (Thermo Scientific). Equal amounts of total proteins
131 were mixed with 4x Laemmli sample buffer and boiled for 10 minutes at 80°C . Protein
132 extracts were separated on SDS-PAGE 7.5% gels and mini-protean III apparatus.
133 GAPDH was used as positive control and to verify equal loading. Proteins were blotted
134 to nitrocellulose membranes using standard Tris-glycine wet method. Membranes
135 were blocked with 5% dry milk (Bio-Rad), incubated with goat polyclonal anti-ACE2
136 (R&D Systems AF3437) at 1/1000 or rabbit polyclonal anti-GAPDH (Protein-Tech,
137 #10494-1-AP) at 1/5000 dilution overnight at 4°C , washed several times in TBST buffer

138 (pH 8.0) and incubated 60 minutes with secondary antibody, anti-goat-HRP (Protein-
139 Tech). Signal was detected using Clarity Max chemiluminescence substrate (Bio-Rad).
140 For confirmation, blots were stripped and re-probed with an additional rabbit
141 monoclonal anti-ACE2 antibody (Abclonal, #A4612). Blots were prepared in three
142 separate experiments with comparable results.

143

144 **ACE2 immunocytochemistry and co-localization analysis**

145 For double immunofluorescence labeling, antigen retrieval procedure was performed
146 on frozen sections cut at 10-12 μ m. Sections were incubated overnight with a mixture
147 of primary goat anti-ACE2 at 1/500 dilution (R&D Systems, #AF3437) and rabbit anti-
148 GnRH (gonadotropin releasing hormone) at 4°C. On the next day, sections were
149 washed five times in PBST (PBS with 0.05% Triton X-100) and incubated with a
150 mixture of secondary anti-rabbit-AF488 antibody and anti-goat-AF594 at 1/500 dilution
151 for 60 minutes at room temperature. Next, sections were stained for 5 minutes at room
152 temperature in Hoechst 33258 (Sigma-Aldrich) to visualize cell nuclei, and sections
153 were then embedded in aqueous antifade medium (Vector laboratories). Alternating
154 cryosections were incubated with rabbit polyclonal anti-CHAT (choline
155 acetyltransferase) instead of rabbit anti-GnRH antibody in the double staining primary
156 antibody mixture. Occasionally, sections were incubated with anti-OMP (olfactory
157 marker protein) at 1/500 dilution in PBST, following the same protocol. After
158 immunocytochemical reactions, sections were analyzed on a Nikon Eclipse 80i
159 microscope and images were taken using a Nikon DP80 camera. Microscopic images
160 were processed using cellSens Dimension 1.13 software (Olympus). Antibodies and
161 vendors are listed in Supplemental Material, Table S1. To compare the signal intensity
162 between nervus terminalis neurons and cells known to express ACE2 and to internalize
163 SARS-CoV-2, the ACE2 fluorescent signal was compared by measuring the optical
164 density of the signal in gray scale (8-bit maps) in ACE2-expressing nervus terminalis
165 neurons and in sustentacular cells of the dorsal olfactory epithelium, using cellSens
166 Dimension 1.13 software (Olympus). Intensity values were defined by regions of
167 interest and a quantitative immunofluorescence score was calculated by comparing
168 the target mean gray intensity for 15 sustentacular cells and 12 GnRH-positive nervus
169 terminalis neurons.

170

171 **Cell counting and statistical analysis**

172 For counting double-labeled neurons, five male wildtype mice at age 3-4 weeks old
173 were used. Approximately every third coronal cryosection (10-12 μm thickness) was
174 stained as described above, and positive neurons were counted in tissue sections
175 under a fluorescent microscope as indicated in Fig. 1 (the medial region from the
176 posterior olfactory epithelium to the caudal end of the olfactory bulb). For each animal,
177 the percentage of double labeled GnRH+/ACE2+ neurons was calculated in relation to
178 the total number of GnRH-positive neurons detected. The same protocol was applied
179 for counting cholinergic nervus terminalis neurons co-labeled with ACE2. A total
180 number of 119 GnRH-positive neurons and a total of 52 CHAT-positive neurons were
181 counted from 3-5 animals, as shown in detail in the Supplemental Material, Table S2.
182 The results were analyzed using GraphPad Prism software. Results are presented as
183 mean \pm standard error of the mean (SEM). An unpaired t-test was applied to determine
184 whether the difference in ACE2 colocalization between GnRH+ and CHAT+ neurons
185 was statistically significant. For details of quantification, see the Supplementary
186 Material, Table S2.

187

188 **TMPRSS2 and cathepsin B and L immunocytochemistry**

189 TMPRSS2 and cathepsins B and L are proteases that SARS-CoV-2 can use to gain
190 entry into host cells (Shang et al., 2020). To determine whether nervus terminalis
191 neurons also express TMPRSS2, tissue sections were incubated with TMPRSS2
192 antibodies at 1:50 or 1:200 dilution as recommended by the manufacturer. We tested
193 one cathepsin B and one cathepsin L antibody and three different anti-TMPRSS2
194 antibodies (listed in the Supplementary Table S1) to determine the presence of these
195 proteases in GnRH-positive nervus terminalis neurons. The same protocol as
196 described above for the ACE2 antibody was used. Quantification of GnRH and
197 cathepsin L co-labeled neurons was performed using the same protocol as described
198 for quantification of neurons labeled with ACE2.

199 **RESULTS**

200

201 It was previously shown that GnRH is a marker for a major fraction of nervus terminalis
202 neurons (Jennes, 1987; Schwanzel-Fukuda et al., 1987; Demski, 1993; Kim et al.,
203 1999; von Bartheld, 2004). Immunolabeling for GnRH in 3-4 week-old mice showed
204 labeled neurons localized along the olfactory nerve between the olfactory epithelium
205 and the olfactory bulbs (Fig. 2A-H), as expected from previous studies in rodents
206 (Schwanzel-Fukuda et al., 1986; Wirsig and Leonard, 1986; Schwanzel-Fukuda et al.,
207 1987). The majority of the GnRH-positive nervus terminalis neurons was located along
208 the midline in the posterior part of the olfactory epithelium and adjacent to the olfactory
209 bulbs. Preliminary examination revealed that these cells were in the same vicinity as
210 cells labeled with the ACE2 antibody (Fig. 2A-B, E-F). The large majority of GnRH-
211 positive nervus terminalis neurons were fusiform and unipolar in shape.

212

213 **Most GnRH⁺ nervus terminalis neurons express ACE2**

214 To determine whether some neurons of the nervus terminalis contained both GnRH
215 and ACE2, and to estimate the number of such neurons, we performed double
216 immunolabeling experiments, and single- and double-labeled cells were counted on
217 15-20 sections from five different animals. The analyzed olfactory epithelium and
218 olfactory bulb region and section's cutting plane are as indicated in Fig. 1. Out of 119
219 GnRH⁺ neurons, 107 (89.9%) were double-labeled for ACE2 (Fig. 3A). The intensity
220 (0-250 scale) of ACE2 immunolabel in nervus terminalis neurons (range of 63 to 114,
221 mean=86) was comparable to the intensity of ACE2 immunolabel (range of 70 to 141,
222 mean=108) that we have previously demonstrated for sustentacular cells in the
223 olfactory epithelium in some of the same tissue sections, and with the same protocol
224 (Bilinska et al., 2020). Controls included omission of the primary antibody (not shown)
225 and double immunofluorescent reactions performed using cryosections derived from
226 an ACE2 knockout mouse as shown in Fig. 2 (I-L). The GnRH-positive neurons were
227 never labeled for olfactory marker protein (OMP), a marker for mature olfactory
228 receptor neurons (Fig. S1, Supplementary Material). The total number of GnRH⁺
229 nervus terminalis neurons per mouse was estimated to be approximately 125, which
230 is very similar to a previous serial section analysis in hamster (about 130-140 GnRH⁺
231 neurons, Wirsig and Leonard, 1986).

232

233 **A small fraction of CHAT⁺ nervus terminalis neurons express ACE2**

234 The nervus terminalis complex is comprised of several distinct heterogeneous
235 populations of neurons. In addition to GnRH neurons which form the major fraction of
236 nervus terminalis neurons, the second largest nervus terminalis subpopulation are
237 cholinergic neurons that can be identified by the presence of choline acetyltransferase
238 (CHAT) or cholinesterase (Wirsig and Leonard, 1986; Demski, 1993; von Bartheld,
239 2004). Therefore, CHAT neurons were also double-labeled with ACE2 and the fraction
240 of CHAT-positive and ACE2-positive neurons was estimated out of a total of 52 CHAT-
241 positive neurons in three animals. In contrast to GnRH⁺/ACE2⁺ cells, only a minor
242 fraction (9.4%) of CHAT-positive neurons were labeled with ACE2 which indicates that
243 relatively few cholinergic nervus terminalis neurons express ACE2 protein (Fig. 3A,
244 Table S2). Most of the CHAT-positive and also ACE2-positive nervus terminalis
245 neurons were fusiform and unipolar in shape. Control experiments included omission
246 of primary antibody (not shown) and double immunofluorescent reactions performed
247 using cryosections derived from ACE2 knockout mouse (see below). The total number
248 of CHAT-positive nervus terminalis neurons per mouse was estimated to be
249 approximately 60-70. This is less than the 130-140 acetylcholinesterase containing
250 nervus terminalis neurons in hamster (Wirsig and Leonard, 1986), but it is known that
251 only a fraction of neurons containing acetylcholinesterase actually are cholinergic
252 (Schwanzel-Fukuda et al., 1986). The difference in colocalization of ACE2 between
253 the two transmitter phenotypes of nervus terminalis neurons was highly significant,
254 indicating that ACE2 expression is not randomly distributed in the nervus terminalis
255 system.

256

257 **Proof of the specificity of the ACE2 antibody: Western blots from ACE2 ^{-/-} mice**

258 Immunolabeling experiments did not reveal any signal beyond background when the
259 primary antibodies were omitted. For more precise visualization of background ACE2
260 staining, tissue derived from ACE2 knock-out mouse was used. In Western blots, the
261 ACE2-specific band was absent in total protein extract obtained from ACE2 ^{-/-} animals
262 (Fig. 3B). Therefore, sections from ACE2 ^{-/-} mice were also used for double
263 immunolabeling experiments with ACE2 antibody and results showed that, as
264 expected, GnRH-positive neurons were negative for ACE2 in tissue sections from the
265 knock-out animals (Fig. 2 I-L).

266

267 **The protease TMPRSS2 is not or minimally expressed in nervus terminalis**
268 **neurons**

269 TMPRSS2 is one of several proteases that cleave the spike protein, allowing SARS-
270 CoV-2 to enter the host cell (Shang et al., 2020). Our attempts to double-label nervus
271 terminalis neurons using three different anti-TMPRSS2 antibodies (Table S1) resulted
272 in no specific label above background in GnRH-positive nervus terminalis neurons
273 (Supplemental Material, Fig. S1E). Levels of TMPRSS2 expression in these neurons
274 may be too low for detection, or TMPRSS2 is not expressed by either the GnRH- or
275 CHAT-expressing nervus terminalis neurons.

276

277 **The proteases cathepsins B and L are expressed in nervus terminalis neurons**

278 It is known that endolysosomal proteases cathepsin B and L can also enhance entry
279 of SARS-CoV-2 to host cells (Gomes et al., 2020; Bollavaram et al., 2021; Zhao et al.,
280 2021). To determine whether some neurons of the nervus terminalis contained both
281 GnRH and cathepsin B or L, and to estimate the number of such cells, we performed
282 double immunolabeling experiments, and single- and double-labeled cells were
283 counted on 15-20 sections from three different animals. The analyzed olfactory
284 epithelium and olfactory bulb region and section's cutting plane are as indicated in Fig.
285 1. After surveying a total of 51 GnRH positive neurons, we found that 90.0% of them
286 were double-labeled for cathepsin L (Cath L, Fig. 3A). A similar trend was observed for
287 cathepsin B with a large proportion of GnRH-positive neurons co-labeled with the two
288 antibodies (data not shown).

289 **DISCUSSION**

290

291 Our experiments confirmed the locations and approximate numbers of GnRH-positive
292 neurons of the nervus terminalis in rodents (Schwanzel-Fukuda et al., 1986; Wirsig
293 and Leonard, 1986; Schwanzel-Fukuda et al., 1987). In mouse, we found that the
294 number of CHAT-positive neurons was about half of the number of GnRH-positive
295 neurons. Interestingly, the large majority of GnRH-positive neurons expressed ACE2
296 and cathepsin B or L, while only a small fraction of CHAT-positive neurons co-localized
297 ACE2. Previous studies have suggested that a larger fraction of the CHAT-positive
298 neurons were multipolar and possibly associated with an autonomic function, while
299 GnRH-positive neurons are thought to be sensory and/or may have neurosecretory
300 functions (Wirsig and Leonard, 1986; Schwanzel-Fukuda et al., 1986).

301

302 Mice have been most often used as model systems for ACE2 expression, for
303 localization of SARS-CoV-2 in the olfactory epithelium, and to study neuro-invasion of
304 the brain along the olfactory route (Butowt and von Bartheld, 2020; Cooper et al., 2020;
305 Rathnasinghe et al., 2020). Mice have the advantage that a large number of mutants
306 are available (Butowt and von Bartheld, 2020), but they normally express an ACE2
307 version that binds SARS-CoV-2 with low affinity (Damas et al., 2020). Therefore, to
308 study SARS-CoV-2 infection in mice, a mouse-adapted virus has to be used (Leist et
309 al., 2020), or mice have to be engineered to express human ACE2 (Butowt et al.,
310 2021).

311

312 SARS-CoV-2 uses ACE2 to bind to host cells, and then the spike protein is cleaved by
313 surface or endosomal proteases to facilitate virus entry. One of the more common
314 proteases to facilitate SARS-CoV-2 entry is TMPRSS2 (Shang et al., 2020). TMPRSS2
315 is minimally expressed in adult neurons (Paoloni-Giacobino et al., 1997), including
316 GnRH-expressing neurons in the brain (Ubuka et al., 2018). Similarly, TMPRSS2 was
317 minimally or not at all expressed in nervus terminalis neurons. TMPRSS2 is only one
318 of several proteases that are known to cleave the spike protein of SARS-CoV-2.
319 Additional proteases that can facilitate SARS-CoV-2 entry into host cells in the absence
320 of TMPRSS2 include cathepsins B and L (Butowt et al., 2020; Gomes et al., 2020;
321 Bollavaram et al., 2021; Zhao et al., 2021), and also furin. Pre-activation by furin
322 enhances viral entry in cells that lack TMPRSS2 or cathepsins, or have low levels of

323 expression of these proteases (Shang et al., 2020). Furin is a ubiquitously expressed
324 protease with a fundamental role in maturation of proteins in the secretory pathway; it
325 is expressed in virtually all cells in rodent brain albeit at different levels (Day et al.,
326 1993). Furin is known to be expressed in Bowman gland cells (Ueha et al., 2021), and
327 therefore would not be a limiting factor for SARS-CoV-2 entry into innervating nervus
328 terminalis neurons. Accordingly, lack of TMPRSS2 in nervus terminalis neurons does
329 not negate the possibility of SARS-CoV-2 infecting these neurons after using
330 alternative proteases to gain entry.

331

332 Our finding of expression of ACE2 and cathepsins B and L in the large majority of
333 GnRH-expressing nervus terminalis neurons suggests that this cranial nerve is a more
334 plausible conduit for brain infection than the olfactory neurons that entirely or for the
335 most part lack ACE2 expression (Butowt and von Bartheld, 2020; Cooper et al., 2020;
336 Klingenstein et al., 2021). The nervus terminalis neurons may obtain the SARS-CoV-
337 2 directly from infected cells in Bowman's glands, or through free nerve endings within
338 the olfactory epithelium, many parts of which degenerate when sustentacular cells are
339 infected by SARS-CoV-2 (Bryche et al., 2020). The lack of ACE2 in olfactory receptor
340 neurons (except for those in the Grueneberg ganglion, Brechbühl et al., 2021) appears
341 to be an effective barrier to virus transfer along the olfactory nerve (Butowt et al., 2021).
342 The nervus terminalis, however, has multiple venues to become infected by the virus,
343 as illustrated in Fig. 4.

344

345 Another important aspect is that the timeline of appearance of SARS-CoV-2 in the
346 brain fits the nervus terminalis projections, with an explosive appearance of the virus
347 in the forebrain in some mouse models (Winkler et al., 2020; Zheng et al., 2020; Zhou
348 et al., 2020; Carossino et al., 2021), rather than a gradual transfer along the olfactory
349 projections as would be expected from a virus that gains access to the brain via
350 olfactory projections (Barnett and Perlman, 1993). The nervus terminalis has direct
351 projections into the forebrain, reaching as far caudal as the hypothalamus (von
352 Bartheld, 2004), and if the virus indeed infects these neurons, this could explain why
353 the virus reaches the brain and cerebrospinal fluid (CSF) spaces much faster than
354 seems possible via "neuron hopping" along olfactory projections. Most of the virus-
355 containing axons in the olfactory nerve demonstrated by de Melo et al. (2021) do not
356 express olfactory marker protein, suggesting that they are not axons belonging to

357 olfactory receptor neurons, and therefore may be nervus terminalis axons which also
358 project along the olfactory nerve (Larsell, 1950).

359

360 On a comparative note, since dolphins and whales have a much larger number of
361 nervus terminalis neurons than any other vertebrates (Oelschläger et al., 1987), and
362 these marine mammals express ACE2 that is highly susceptible to SARS-CoV-2
363 binding (Damas et al., 2020), our finding of ACE2 in nervus terminalis neurons
364 suggests that these animals may be more vulnerable to brain infection via the nervus
365 terminalis – even in the absence of an olfactory system.

366

367 In humans, the number of nervus terminalis neurons is relatively small (a few hundred
368 to a few thousand neurons depending on age, Brookover, 1917; Larsell, 1950; Jin et
369 al., 2019). However, it is possible that such a relatively small number is sufficient to
370 mediate viral infection. The nervus terminalis directly innervates secretory cells of the
371 Bowman's glands (Larsell, 1950) that are known to express ACE2 (Brann et al., 2020;
372 Chen et al., 2020; Cooper et al., 2020; Ye et al., 2020; Zhang et al., 2020; Klingenstein
373 et al., 2021) and readily become infected with SARS-CoV-2 (Ye et al., 2020; Leist et
374 al., 2020; Meinhardt et al., 2020; Zhang et al., 2020; Zheng et al., 2020) (Fig. 4). In
375 addition, the nervus terminalis has many free nerve endings within the olfactory
376 epithelium (Larsell, 1950) – an epithelium that is heavily damaged when ACE2-
377 expressing sustentacular cells become infected and degenerate (Bryche et al., 2020).
378 Finally, a major component of the nervus terminalis innervates blood vessels below
379 the olfactory epithelium and projects via cerebrospinal fluid (CSF)-containing spaces
380 (Larsell, 1950; Jennes, 1987). Some nervus terminalis neurons have direct projections
381 to the hypothalamus (Pearson, 1941; Larsell, 1950; von Bartheld, 2004), a brain region
382 that may serve as a hub for virus spread throughout the brain (Nampoothiri et al., 2020;
383 Zheng et al., 2020).

384

385 Another argument to consider the nervus terminalis as an alternative to the olfactory
386 route is that neuro-invasion in most animal models is highly variable, even in the same
387 species and transgenic model (Jiang et al., 2020; Oladunni et al., 2020; Rathnasinghe
388 et al., 2020; Winkler et al., 2020; Ye et al., 2020; Zheng et al., 2020; Zhou et al., 2020),
389 and this is in contrast to the olfactory system that is consistent in terms of numbers of

390 neurons, gene expression and projections. The nervus terminalis, on the other hand,
391 is known for its large variability between individuals of the same species or even when
392 comparing the right side with the left side of the same individual (Larsell, 1918; Jin et
393 al., 2019). Such numerical differences can approach or even exceed an entire order of
394 magnitude (Schwanzel-Fukuda et al., 1987; Jin et al., 2019) – and thus may explain
395 the reported large variability in neuro-invasion (Butowt et al., 2021). Taken together,
396 nervus terminalis neurons, for the above reasons, should be considered as a plausible
397 alternative to the olfactory projections for neuro-invasion of SARS-CoV-2 from the nose
398 to the brain in COVID-19. Whether the virus can indeed infect nervus terminalis
399 neurons cannot be deduced by protein expression, but has to be determined by
400 experiments using infectious SARS-CoV-2 after nasal inoculation in experimental
401 animal models, or by demonstration of SARS-CoV-2 in nervus terminalis neurons in
402 tissues from patients with COVID-19.

403

404

405 **ACKNOWLEDGMENTS**

406 Supported by the “Excellence Initiative-Research University” programme at the
407 Nicolaus Copernicus University (R.B.), and grant GM103554 from the National
408 Institutes of Health (C.S.v.B.).

409

410 **CONTRIBUTION TO THE FIELD**

411

412 The new coronavirus responsible for the COVID-19 pandemic can infect the brain in
413 humans and in some animal models. It is currently not known how this virus infects the
414 brain. Many researchers believe that the virus enters the brain by using a route along
415 the olfactory nerve. However, the olfactory neurons in the nose do not express the
416 obligatory virus entry receptors, and the timing of arrival and transfer of the virus in
417 brain targets is inconsistent with a neuronal transfer along olfactory projections. Here
418 we show that an alternative route for the new coronavirus to infect the brain is more
419 plausible. We show that many nervus terminalis neurons express the spike-binding
420 virus entry protein. Since these neurons have direct synaptic contact with cells known
421 to become infected in the nose, and have direct projections to various targets in the
422 forebrain, the nervus terminalis neurons may provide an alternative route for the new
423 coronavirus to gain access from the nose to the brain. The main contribution of our
424 paper is to show that a plausible alternative route to brain infection exists that needs
425 to be pursued by examination of human tissues and by testing in appropriate animal
426 models whether the new coronavirus indeed utilizes this pathway.

427 **REFERENCES**

428
429
430
431
432
433
434
435
436
437
438
439
440
441
442
443
444
445
446
447
448
449
450
451
452
453
454
455
456
457
458
459
460
461
462
463
464
465
466
467
468
469
470
471
472
473
474
475
476

Barnett, E.M., and Perlman, S. (1993). The olfactory nerve and not the trigeminal nerve is the major site of CNS entry for mouse hepatitis virus, strain JHM. *Virology*. 194(1), 185-191.

Barnett, E.M., Evans, G.D., Sun, N., Perlman, S., and Cassell, M.D. (1995). Anterograde tracing of trigeminal afferent pathways from the murine tooth pulp to cortex using herpes simplex virus type 1. *J Neurosci*. (4), 2972-2984.

Bilinska, K., Jakubowska, P., Von Bartheld, C.S., and Butowt, R. (2020). Expression of the SARS-CoV-2 Entry Proteins, ACE2 and TMPRSS2, in Cells of the Olfactory Epithelium: Identification of Cell Types and Trends with Age. *ACS Chem Neurosci*. 11(11), 1555-1562.

Bollavaram, K., Leeman, T. H., Lee, M. W., Kulkarni, A., Upshaw, S. G., Yang, J., et al. (2021). Multiple sites on SARS-CoV-2 spike protein are susceptible to proteolysis by cathepsins B, K, L, S, and V. *Protein Sci*. 2021 Jun;30(6):1131-1143.

Bougakov, D., Podell, K., and Goldberg, E. (2020). Multiple Neuroinvasive Pathways in COVID-19. *Mol Neurobiol*. 29,1–12.

Briguglio, M., Bona, A., Porta, M., Dell'Osso, B., Pregliasco, F.E., and Banfi, G. (2020). Disentangling the hypothesis of host dysosmia and SARS-CoV-2: The bait symptom that hides neglected neurophysiological routes. *Front Physiol*. 11, 671.

Brann, D.H., Tsukahara, T., Weinreb, C., Lipovsek, M., Van den Berge, K., Gong, B., et al. (2020). Non-neuronal expression of SARS-CoV-2 entry genes in the olfactory system suggests mechanisms underlying COVID-19-associated anosmia. *Sci Adv*. 6(31):eabc5801.

Brechbühl, J., Wood, D., Bouteiller, S., Lopes, A.C., Verdumo, C., and Broillet, M.-C. (2021). Age-dependent appearance of SARS-CoV-2 entry cells in mouse chemosensory systems reflects COVID-19 anosmia and ageusia symptoms. *bioRxiv* [Preprint] March 29, 2021 doi: <https://doi.org/10.1101/2021.03.29.437530>.

Brookover, C. (1917). The peripheral distribution of the nervus terminalis in an infant. *J Comp Neurol*. 28, 349-360.

Bryche, B., St Albin, A., Murri, S., Lacôte, S., Pulido, C., Ar Gouilh, M., et al. (2020). Massive transient damage of the olfactory epithelium associated with infection of sustentacular cells by SARS-CoV-2 in golden Syrian hamsters. *Brain Behav Immun*. 89, 579-586.

Burks, S.M., Rosas-Hernandez, H., Alenjandro Ramirez-Lee, M., Cuevas, E., and Talpos, J.C. (2021). Can SARS-CoV-2 infect the central nervous system via the olfactory bulb or the blood-brain barrier? *Brain Behav Immun*. 20, 32489-32492.

- 477 Butowt, R., and Bilinska, K. (2020). SARS-CoV-2: Olfaction, Brain Infection, and the
478 Urgent Need for Clinical Samples Allowing Earlier Virus Detection. *ACS Chem*
479 *Neurosci.* 11(9),1200-1203.
480
- 481 Butowt, R., and von Bartheld, C.S. (2020). Anosmia in COVID-19: Underlying
482 Mechanisms and Assessment of an Olfactory Route to Brain Infection. *Neuroscientist.*
483 doi: 10.1177/1073858420956905. Epub ahead of print.
484
- 485 Butowt, R., Pyrc, K., and von Bartheld, C.S. (2020). Battle at the entrance gate: CIITA
486 as a weapon to prevent the internalization of SARS-CoV-2 and Ebola viruses. *Signal*
487 *Transduct Target Ther.* Nov 24;5(1):278.
488
- 489 Butowt, R., Meunier, N., Bryche, B., and von Bartheld, C.S. (2021). The olfactory nerve
490 is not a likely route to brain infection in COVID-19: a critical review of data from humans
491 and animal models. *Acta Neuropathol*, 1–14. Advance online publication.
492 <https://doi.org/10.1007/s00401-021-02314-2>.
493
- 494 Carossino, M., Montanaro, P., O'Connell, A., Kenney, D., Gertje, H., Grosz, K.A., et al.
495 (2021). Fatal neuroinvasion of SARS-CoV-2 in K18-hACE2 mice is partially dependent
496 on hACE2 expression. *bioRxiv [Preprint]* doi: 10.1101/2021.01.13.425144. (accessed
497 on May 30, 2021).
498
- 499 Chen, M., Shen, W., Rowan, N. R., Kulaga, H., Hillel, A., Ramanathan, M., Jr, et al.
500 (2020). Elevated ACE-2 expression in the olfactory neuroepithelium: implications for
501 anosmia and upper respiratory SARS-CoV-2 entry and replication. *Eur Resp J.* 56(3),
502 2001948.
503
- 504 Cooper, K.W., Brann, D.H., Farruggia, M.C., Bhutani, S., Pellegrino, R., Tsukahara, T.,
505 et al. (2020). COVID-19 and the Chemical Senses: Supporting Players Take Center
506 Stage. *Neuron.* 107(2), 219-233.
507
- 508 Damas, J., Hughes, G.M., Keough, K.C., Painter, C.A., Persky, N.S., Corbo, M., et al.
509 (2020). Broad host range of SARS-CoV-2 predicted by comparative and structural
510 analysis of ACE2 in vertebrates. *Proc Natl Acad Sci U S A.* 117(36), 22311-22322.
511
- 512 Day, R., Schafer, M.K., Cullinan, W.E., Watson, S.J., Chrétien, M., Seidah, N.G.
513 (1993). Region specific expression of furin mRNA in the rat brain. *Neurosci Lett.*
514 149(1), 27-30.
515
- 516 de Melo, G.D., Lazarini, F., Levallois, S., Hautefort, C., Michel, V., Larrous, F., et al.
517 (2021). COVID-19-related anosmia is associated with viral persistence and
518 inflammation in human olfactory epithelium and brain infection in hamsters. *Sci Transl*
519 *Med*, eabf8396. E-pub. <https://doi.org/10.1126/scitranslmed.abf8396>.
520
- 521 Demski, L.S. (1993). Terminal nerve complex. *Acta Anat (Basel).* 148(2-3), 81-95.
522
- 523 Dubé, M., Le Coupand, A., Wong, A.H.M., Rini, J.M., Desforages, M., and Talbot, P.J.
524 (2018). Axonal Transport Enables Neuron-to-Neuron Propagation of Human
525 Coronavirus OC43. *J Virol.* 92(17), 404-418.

- 526 Ellul, M.A., Benjamin, L., Singh, B., Lant, S., Michael, B.D., Easton, A., et al. (2020).
527 Neurological associations of COVID-19. *Lancet Neurol.* 19(9), 767-783.
528
- 529 Gomes, C. P., Fernandes, D. E., Casimiro, F., da Mata, G. F., Passos, M. T., Varela,
530 P., et al. (2020). Cathepsin L in COVID-19: From Pharmacological Evidences to
531 Genetics. *Front Cell Infect Microbiol.* Dec 8;10:589505.
532
- 533 Jennes, L. (1987). The nervus terminalis in the mouse: light and electron microscopic
534 immunocytochemical studies. *Ann N Y Acad Sci.* 519,165-173.
535
- 536 Jiang, R. D., Liu, M. Q., Chen, Y., Shan, C., Zhou, Y. W., Shen, X. R., et al. (2020).
537 Pathogenesis of SARS-CoV-2 in Transgenic Mice Expressing Human Angiotensin-
538 Converting Enzyme 2. *Cell.* 182(1), 50–58.e8.
539
- 540 Jin, Z.W., Cho, K.H., Shibata, S., Yamamoto, M., Murakami, G., and Rodríguez-
541 Vázquez, J.F. (2019). Nervus terminalis and nerves to the vomeronasal organ: a study
542 using human fetal specimens. *Anat Cell Biol.* 52(3), 278-285.
543
- 544 Kim, K.H., Patel, L., Tobet, S.A., King, J.C., Rubin, B.S., and Stopa, E.G. (1999).
545 Gonadotropin-releasing hormone immunoreactivity in the adult and fetal human
546 olfactory system. *Brain Res.* 826(2), 220-229.
547
- 548 Klingenstein, M., Klingenstein, S., Neckel, P.H., Mack, A.F., Wagner, A.P, Kleger, A.,
549 et al. (2021). Evidence of SARS-CoV2 Entry Protein ACE2 in the Human Nose and
550 Olfactory Bulb. *Cells Tissues Organs* 209(4-6), 155-164.
551
- 552 Larsell, O. (1918). Nervus terminalis: mammals. *J Comp Neurol.* 30, 3-68.
553
- 554 Larsell, O. (1950). The nervus terminalis. *Ann Otol Rhinol Laryngol.* 59(2), 414-438.
555
- 556 Leist, S.R., Dinnon, K.H., Schäfer, A., Tse, L.V., Okuda, K., Hou, Y.J., et al. (2020). A
557 Mouse-Adapted SARS-CoV-2 Induces Acute Lung Injury and Mortality in Standard
558 Laboratory Mice. *Cell.* 183 (4),1070-1085.
559
- 560 Li, Z., Liu, T., Yang, N., Han, D., Mi, X., Li, Y., et al. (2020). Neurological manifestations
561 of patients with COVID-19: potential routes of SARS-CoV-2 neuroinvasion from the
562 periphery to the brain. *Front Med.* 14(5), 533-541.
563
- 564 Liang, F. (2020). Sustentacular Cell Enwrapment of Olfactory Receptor Neuronal
565 Dendrites: An Update. *Genes (Basel).* 11(5), 493.
566
- 567 Masre, S.F., Jufri, N.F., Ibrahim, F.W., and Abdul Raub, S.H. (2020). Classical and
568 alternative receptors for SARS-CoV-2 therapeutic strategy. *Rev Med Virol.* e2207.
569 Advance online publication. <https://doi.org/10.1002/rmv.2207>.
570
- 571 Matschke, J., Lütgehetmann, M., Hagel, C., Sperhake, J.P., Schröder, A.S., Edler, C.,
572 et al. (2020). Neuropathology of patients with COVID-19 in Germany: a post-mortem
573 case series. *Lancet Neurol.* 19(11), 919-929.
574

- 575 Meinhardt, J., Radke, J., Dittmayer, C., Franz, J., Thomas, C., Mothes, R., et al. (2021).
576 Olfactory transmucosal SARS-CoV-2 invasion as a port of central nervous system
577 entry in individuals with COVID-19. *Nat Neurosci.* 24(2), 168-175.
578
- 579 Mukerji, S.S., and Solomon, I.H. (2021). What can we learn from brain autopsy in
580 COVID-19? *Neurosci Lett.* 742:135528. doi: 10.1016/j.neulet.2020.135528.
581
- 582 Nampoothiri, S., Sauve, S., Ternier, G., Fernandois, D., Coelho, C., Imbernon, M., et
583 al. (2020). The hypothalamus as a hub for putative SARS-CoV-2 brain infection.
584 *bioRxiv [Preprint]* doi: <https://doi.org/10.1101/2020.06.08.139329>. (accessed on May
585 30, 2021)
586
- 587 Natoli, S., Oliveira, V., Calabresi, P., Maia, L.F., and Pisani, A. (2020). Does SARS-
588 Cov-2 invade the brain? Translational lessons from animal models. *Eur J Neurol.*
589 9,1764-1773.
590
- 591 Netland, J., Meyerholz, D.K., Moore, S., Cassell, M., and Perlman, S. (2008). Severe
592 acute respiratory syndrome coronavirus infection causes neuronal death in the
593 absence of encephalitis in mice transgenic for human ACE2. *J Virol.* 82(15), 7264-
594 7275.
595
- 596 Oelschläger, H.A., Buhl, E.H., and Dann, J.F. (1987). Development of the nervus
597 terminalis in mammals including toothed whales and humans. *Ann N Y Acad Sci.* 519,
598 447-464.
599
- 600 Oladunni, F. S., Park, J. G., Pino, P. A., Gonzalez, O., Akhter, A., Allué-Guardia, A., et
601 al. (2020). Lethality of SARS-CoV-2 infection in K18 human angiotensin-converting
602 enzyme 2 transgenic mice. *Nat Commun.* 11(1), 6122.
603
- 604 Paoloni-Giacobino, A., Chen, H., Peitsch, M. C., Rossier, C., and Antonarakis, S.E.
605 (1997). Cloning of the TMPRSS2 gene, which encodes a novel serine protease with
606 transmembrane, LDLRA, and SRCR domains and maps to 21q22.3. *Genomics,* 44(3),
607 309–320.
608
- 609 Pearson, A.A. (1941). The development of the nervus terminalis in man. *J Comp*
610 *Neurol.* 75, 39-66.
611
- 612 Rathnasinghe, R., Strohmeier, S., Amanat, F., Gillespie, V.L., Krammer, F., García-
613 Sastre, A., et al. (2020). Comparison of transgenic and adenovirus hACE2 mouse
614 models for SARS-CoV-2 infection. *Emerg Microbes Infect.* 1, 2433-2445.
615
- 616 Ridgway, S.H., Demski, L.S., Bullock, T.H., and Schwanzel-Fukuda, M. (1987). The
617 terminal nerve in odontocete cetaceans. *Ann N Y Acad Sci.* 519, 201-212.
618
- 619 Schwanzel-Fukuda, M., Morrell, J. I., and Pfaff, D. W. (1986). Localization of choline
620 acetyltransferase and vasoactive intestinal polypeptide-like immunoreactivity in the
621 nervus terminalis of the fetal and neonatal rat. *Peptides.* 7(5), 899–906.
622

- 623 Schwanzel-Fukuda, M., Garcia, M.S., Morrell, J.I., and Pfaff, D.W. (1987). Distribution
624 of luteinizing hormone-releasing hormone in the nervus terminalis and brain of the
625 mouse detected by immunocytochemistry. *J Comp Neurol.* 255(2), 231-244.
626
- 627 Shang, J., Wan, Y., Luo, C., Ye, G., Geng, Q., Auerbach, A., and Li, F. (2020). Cell
628 entry mechanisms of SARS-CoV-2. *Proc Natl Acad Sci USA*, 117(21), 11727–11734.
629
- 630 Solomon, T. (2021). Neurological infection with SARS-CoV-2 - the story so far. *Nat*
631 *Rev Neurol.* 1–2.
632
- 633 Thakur, K.T., Miller, E.H., Glendinning, M.D., Al-Dalahmah, O., Banu, M.A., Boehme,
634 A.K., et al. (2021). COVID-19 neuropathology at Columbia University Irving Medical
635 Center/New York Presbyterian Hospital. *Brain*, awab148. Advance online publication.
636 <https://doi.org/10.1093/brain/awab148>.
637
- 638 Tikellis, C., and Thomas, M.C. (2012). Angiotensin-Converting Enzyme 2 (ACE2) Is a
639 Key Modulator of the Renin Angiotensin System in Health and Disease. *Int J Pept.*
640 2012:256294.
641
- 642 Ubuka, T., Moriya, S., Soga, T., and Parhar, I. (2018). Identification of Transmembrane
643 Protease Serine 2 and Forkhead Box A1 As the Potential Bisphenol A Responsive
644 Genes in the Neonatal Male Rat Brain. *Front Endocrinol*, 9, 139.
645
- 646 Ueha, R., Kondo, K., Kagoya, R., Shichino, S., Shichino, S., and Yamasoba, T. (2021).
647 ACE2, TMPRSS2, and Furin expression in the nose and olfactory bulb in mice and
648 humans. *Rhinology*, 59(1), 105–109.
649
- 650 van Riel, D., Verdijk, R., and Kuiken, T. (2015). The olfactory nerve: a shortcut for
651 influenza and other viral diseases into the central nervous system. *J Pathol.* 235(2),
652 277-287.
653
- 654 von Bartheld, C.S. (2004). The terminal nerve and its relation with extrabulbar
655 "olfactory" projections: lessons from lampreys and lungfishes. *Microsc Res Tech.* 65(1-
656 2), 13-24.
657
- 658 Winkler, E. S., Bailey, A. L., Kafai, N. M., Nair, S., McCune, B. T., Yu, J., et al. (2020).
659 SARS-CoV-2 infection of human ACE2-transgenic mice causes severe lung
660 inflammation and impaired function. *Nat Immunol.* 21(11), 1327–1335.
661
- 662 Wirsig, C.R., and Leonard, C.M. (1986). Acetylcholinesterase and luteinizing hormone-
663 releasing hormone distinguish separate populations of terminal nerve neurons.
664 *Neuroscience*, 19(3), 719–740.
665
- 666 Ye, Q., Zhou, J., Yang, G., Li, R.-T., He, Q., Zhang, Y., et al. (2020). SARS-CoV-2
667 infection causes transient olfactory dysfunction in mice. *bioRxiv [Preprint]* doi:
668 <https://doi.org/10.1101/2020.11.10.376673>. (accessed on May 30, 2021).
669
- 670 Zhang, A.J., Lee, A.C., Chu, H., Chan, J.F., Fan, Z., Li, C., et al. (2020). SARS-CoV-2
671 infects and damages the mature and immature olfactory sensory neurons of hamsters.
672 *Clin Infect Dis.* 15:ciaa995. doi: 10.1093/cid/ciaa995

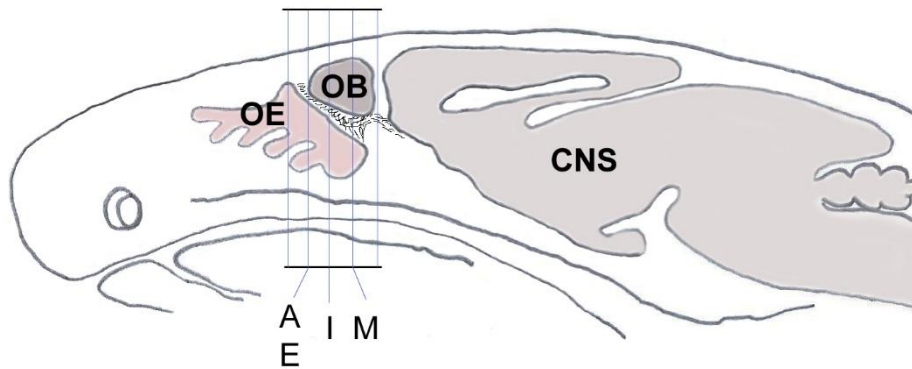
673
674 Zhao, M.M., Yang, W.L., Yang, F.Y., Zhang, L., Huang, W.J., Hou, W., et al. (2021).
675 Cathepsin L plays a key role in SARS-CoV-2 infection in humans and humanized mice
676 and is a promising target for new drug development. *Signal Transduct Target Ther.*
677 Mar 27;6(1):134.
678
679 Zheng, J., Wong, L.R., Li, K., Verma, A.K., Ortiz, M., Wohlford-Lenane, C., et al.
680 (2021). COVID-19 treatments and pathogenesis including anosmia in K18-hACE2
681 mice. *Nature* 589, 603–607.
682
683 Zhou, B., Thao, T.T.N., Hoffmann, D., Taddeo, A., Ebert, N., Labroussaa, F., et al.
684 (2020). SARS-CoV-2 spike D614G variant confers enhanced replication and
685 transmissibility. *bioRxiv* [Preprint]. doi: 10.1101/2020.10.27.357558. (accessed on
686 May 30, 2021).
687
688 Zubair, A.S., McAlpine, L.S., Gardin, T., Farhadian, S., Kuruvilla, D.E., and Spudich,
689 S. (2020). Neuropathogenesis and Neurologic Manifestations of the Coronaviruses in
690 the Age of Coronavirus Disease 2019: A Review. *JAMA Neurol.* 77(8), 1018-1027.
691

692 **FIGURES AND FIGURE LEGENDS**

693

694

695



696

697

698 **Fig. 1.** Schematic sagittal section through a mouse head shows the orientation and
699 planes of tissue sections from Fig. 2A, E, I and M. Sections within those planes were
700 used for demonstration of double-immunolabeling and for cell counting. CNS, central
701 nervous system; OB, olfactory bulb; OE, olfactory epithelium.

702

703

704

705

706

707

708

709

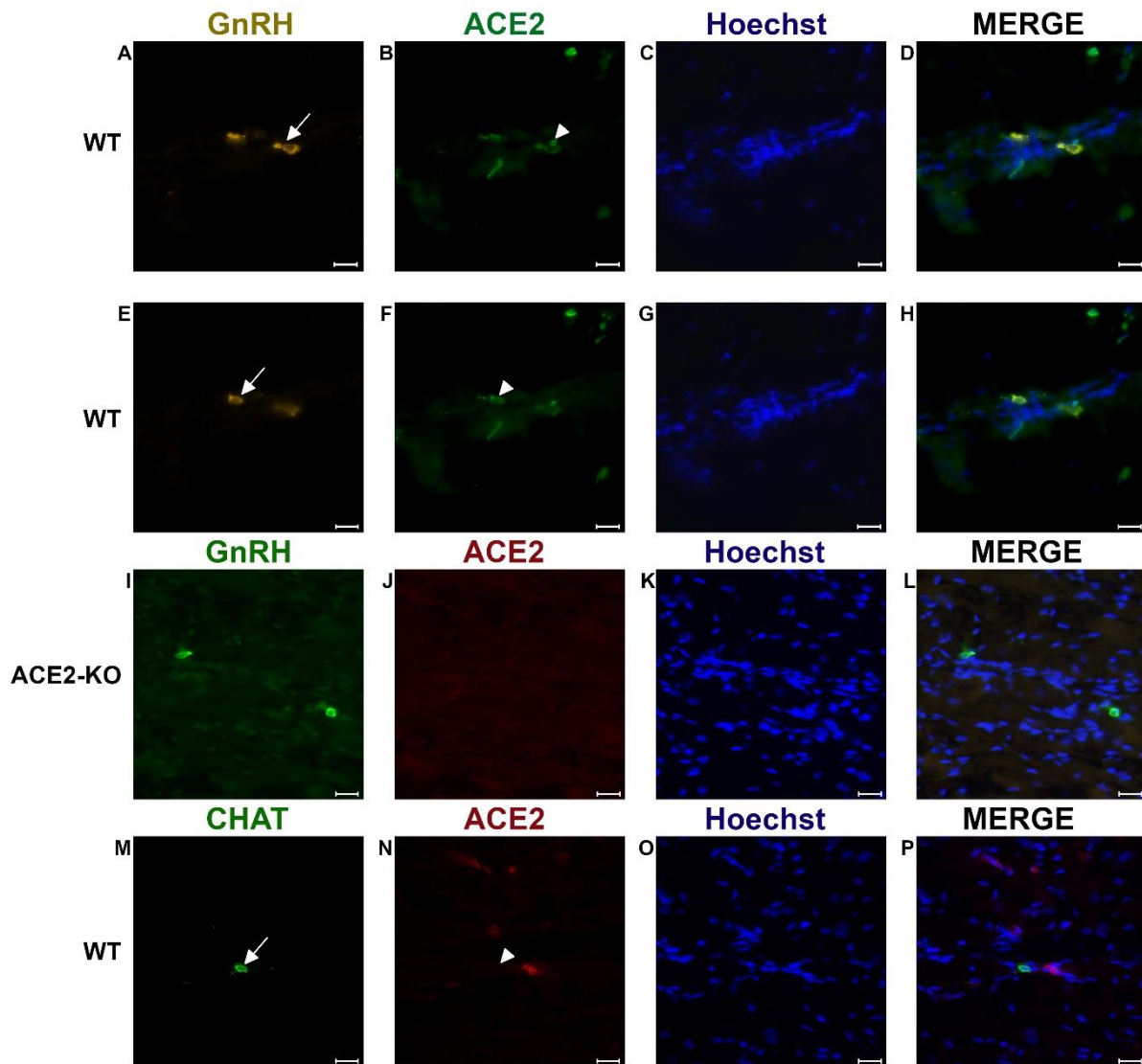
710

711

712

713

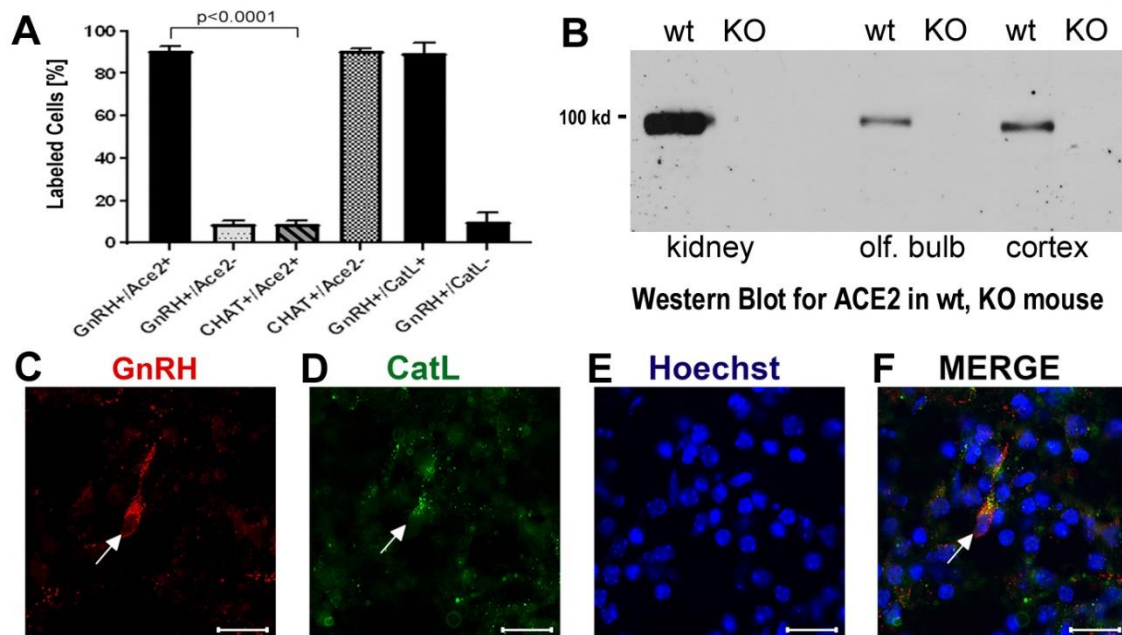
714



715

716 **Fig. 2.** Examples of double immunofluorescent labeling for nervus terminalis
717 neuronal markers GnRH (**A, E**) or CHAT (**M**) and ACE2 (**B, F, J, N**) in the medial
718 region adjacent to the olfactory bulbs as indicated in Fig. 1. Panels **A-D** and **E-H**
719 show slightly different focal planes to demonstrate the morphology of the two or three
720 different neurons. Nuclei are stained with Hoechst 33258 (**C, G, K, O**). Merged
721 images are shown in the last column (**D, H, L, P**). The neuronal somas labeled with
722 GnRH (**A, E**) are co-labeled with ACE2 (**B, F**) as shown after merging (**D, H**). GnRH
723 positive cells in the ACE2 knock-out mouse (**I**) are not labeled with ACE2 (**J**). The
724 majority of cholinergic neurons are not labeled with ACE2 (**M, N**), as quantified in Fig.
725 3A. Control sections probed without primary antibodies or with control rabbit IgG had
726 no detectable signal (not shown). Arrows and triangles indicate double-labeled
727 neurons or lack thereof. Scale bars: 20 μ m.

728



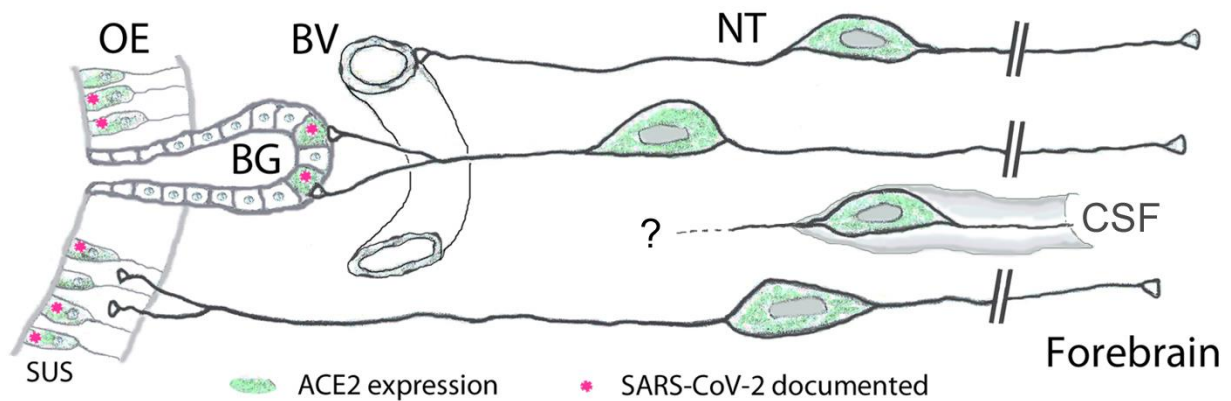
729

730

731 **Fig. 3A-F.** Quantification of neurons labeled with nervus terminalis markers, virus
732 entry proteins, and verification of the specificity of the ACE2 antibody.

733 **A.** The large majority of GnRH-positive neurons is also ACE2-positive. In contrast,
734 the majority of CHAT-positive (cholinergic) nervus terminalis neurons lack ACE2-
735 expression. The total number of counted GnRH-positive or CHAT-positive neurons
736 was set at 100%. Error bars represent \pm SEM. A t-test shows that the colocalization
737 difference between GnRH- and CHAT-positive nervus terminalis neurons is
738 significant at $p < 0.0001$. For further details, see Table S2. **B.** Western blot of ACE2 in
739 wildtype (wt) mice and in ACE2 knock-out (KO) mice. The first two lanes (kidney)
740 were loaded with 25 μ g total protein, the lanes for olfactory bulb and cerebral cortex
741 were loaded with 60 μ g total protein, and probed with the R&D ACE2 antibody. No
742 ACE2 protein was detectable in the ACE2 KO mice, proving that the antibody indeed
743 recognizes ACE2. **C-F.** Example of GnRH-positive nervus terminalis neurons which
744 are also cathepsin L-positive. **C.** One GnRH-labeled neuron is marked with a white
745 arrow. **D.** The same neuron is labeled with the cathepsin L antibody (CatL, white
746 arrow). **E.** The cell nuclei are stained with Hoechst nuclear dye. **F.** The three images
747 are merged to show co-localization in the neuron indicated with the white arrow. All
748 scale bars are 20 μ m.

749



750

751

752 **Fig. 4.** Peripheral projections of nervus terminalis (NT) neurons and their
753 presumptive relationship with ACE2-expressing neurons in the olfactory epithelium
754 and known SARS-CoV-2 infection. NT neurons innervate blood vessels (BV),
755 Bowman gland (BG) cells, the olfactory epithelium (OE), and contact cerebrospinal
756 fluid (CSF) spaces. Peripheral projections of NT neurons according to Larsell (1950),
757 CSF contacts according to Jennes (1987). Cells expressing ACE2 are indicated in
758 green, including sustentacular cells (SUS) and BG cells. Both of these cell types
759 have been shown to express ACE2 (Bilinska et al., 2020; Brann et al., 2020; Chen et
760 al., 2020; Ye et al., 2020; Zhang et al., 2020; Klingenstein et al., 2021). Cell types
761 that have been documented to be infected by SARS-CoV-2 are indicated with pink
762 asterisks. SARS-CoV-2 localization in SUS cells according to Bryche et al., 2020;
763 Leist et al., 2020; Ye et al., 2020; Zhang et al., 2020; Zheng et al., 2020; de Melo et
764 al., 2021, and in BG cells according to Bryche et al., 2020; Leist et al., 2020; Ye et
765 al., 2020. BG cells furthermore express the protease furin (Ueha et al., 2021) which
766 may facilitate virus entry into those nervus terminalis neurons which innervate BG
767 cells.

768

769

770 **SUPPLEMENTARY MATERIAL**

771

772 **SUPPLEMENTAL TABLES**

773

774 **Table S1.** Primary and secondary antibodies used in this study.

Primary antibodies	Company	Catalog #	Type
ACE2	R&D Systems	AF3437	goat polyclonal
ACE2	ABclonal	A4612	rabbit monoclonal
Cathepsin B	R&D Systems	AF965	goat polyclonal
Cathepsin L	R&D Systems	AF1515	goat polyclonal
CHAT	Proteintech	24418-1-AP	rabbit polyclonal
GnRH1	Proteintech	26950-1-AP	rabbit polyclonal
OMP	WAKO	544-10001	goat polyclonal
TMPRSS2	Novus Biologicals	NBP3-00492	rabbit monoclonal
TMPRSS2	Abcam	ab242384	rabbit monoclonal
TMPRSS2	St John's	STJ11102428	rabbit monoclonal
Secondary antibodies			Fluorescent conjugate
donkey anti-rabbit	Abcam	ab15006	Alexa Fluor 488
donkey anti-goat	Abcam	ab150136	Alexa Fluor 594
horse anti-rabbit	Vector	DI-1094	Alexa Fluor 594
horse anti-goat	Vector	DI-3088	Alexa Fluor 488

775

776 Abbreviations: ACE2, angiotensin converting enzyme 2; CHAT, choline acetyltransferase; GnRH1,
777 gonadotropin releasing hormone 1; OMP, olfactory marker protein; TMPRSS2, transmembrane
778 protease serine 2.

779

780 **TABLE S2.** Numbers of animals, sections, and numbers of neurons double-labeled for
781 nervus terminalis markers (GnRH, CHAT) and ACE2.

	# of sections	# of GnRH neurons	# of GnRH and ACE2	%
GnRH and ACE2				
Mouse 1	16	25	23	92.0
Mouse 2	21	30	27	90.0
Mouse 3	15	21	19	90.5
Mouse 4	11	10	8	80.0
Mouse 5	22	33	30	90.9
Sum/mean	85	119	107	89.9
CHAT and ACE2				
Mouse 1	21	20	2	10.0
Mouse 2	15	18	2	11.1
Mouse 3	18	14	1	7.1
Sum/mean	54	52	5	9.4
t-test				p<0.0001

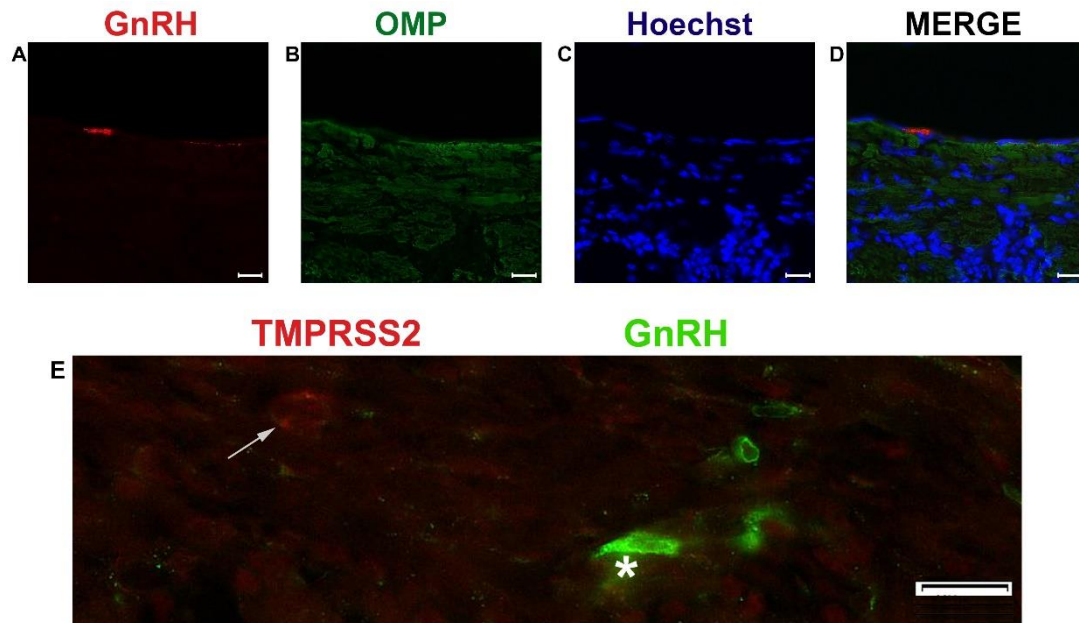
782

783 **SUPPLEMENTAL FIGURES**

784

785

786



787

788

789 **Fig. S1.** Examples of double immunofluorescent labeling of nervus terminalis
790 neurons with the markers GnRH and olfactory marker protein (OMP) (A-D), and
791 GnRH and TMPRSS2 (E). Label for GnRH (A) and OMP (B) in the medial region
792 adjacent to the olfactory bulbs as indicated in Fig. 1. Nuclei are stained with Hoechst
793 33258 (C) and the merged image is shown in (D). GnRH-labeled cells were never
794 labeled for OMP in this region. (E) GnRH-labeled nervus terminalis neurons (one
795 neuron indicated with the white asterisk) did not co-localize with cells positive for
796 TMPRSS2 (white arrow). Scale bars: 20 μ m.